Microphase Separation of Hybrid Dendron−Linear Diblock Copolymers into Ordered Structures

Michael E. Mackay*

Department of Chemical Engineering and Materials Science, Michigan State University, East Lansing, Michigan 48824

Ye Hong and Miyoun Jeong

Department of Chemical, Biochemical and Materials Engineering, Stevens Institute of Technology, Castle Point on the Hudson, Hoboken, New Jersey 07030

Brian M. Tande and Norman J. Wagner

Center for Molecular and Engineering Thermodynamics, Department of Chemical Engineering, University of Delaware, Newark, Delaware 19716

Sheng Hong and Samuel P. Gido

Polymer Science and Engineering Department, University of Massachusetts Amherst, Amherst, Massachusetts 01003

Robert Vestberg and Craig J. Hawker

IBM-Almaden Research Center, 650 Harry Road, San Jose, California 95120

Received March 22, 2002; Revised Manuscript Received July 26, 2002

ABSTRACT: Hybrid copolymers with dendritic−linear blocks are shown to exhibit many of the classic microphase-separated structures of linear−linear block copolymers. Transmission electron microscopy (TEM), small-angle X-ray scattering (SAXS), and small-angle neutron scattering (SANS) were used to evaluate the morphology of a sixth generation (G6) poly(benzyl ether) dendron covalently bonded to linear polystyrene (PS) at the dendron focal point. Increasing the fraction of the linear block, ϕ_{PS}, through an increase in the molecular weight of the PS block revealed morphologies evolving from disordered to ordered lamellar to hexagonally close-packed dendron cylinders. Significantly, the observed morphologies are distinct from those expected for analogous linear−linear blocks at equivalent volume fraction, although the direction of progression follows expectation. Quantitative analysis suggests substantial molecular deformation or shape change in the dendritic phase. The possible role of conformational entropy in determining the overall free energy is suggested to be important for this class of block copolymer.

Introduction

Microphase separation of block copolymers into ordered phases has been the subject of intense research over the past two decades.[1,2] Much has been learned for linear−linear block systems, and recent attention has shifted to the effect of molecular architecture on this phase behavior.[3−6] These new systems, typically star polymers, show similar morphologies to the linear−linear systems with the appearance of lamellar and cylinder morphologies. However, recent work has shown that some star−block systems exhibit qualitative differences in comparison to their linear analogues, with lamellar structures having a longer period than expected.[7] This was explained by extra stretching of chains near the interface. Other block copolymer systems containing molecular architectures such as hyperbranched or dendritic polymers may exhibit qualitatively different microstructures and thus provides motivation for this study.

Dendritic macromolecules are incapable of displaying classic chain stretching although it has been shown they can alter their size through variation in the solvent quality.[8] In fact, the viscosimetric volume of dendrons has been reported to decrease by a factor of 2 upon change in solvent quality, leading to a single molecule density (ρ_m) in poorer solvents close to that of the bulk (ρ).[9] In this condition, the intrinsic viscosity ($[\eta]$, $\rho_m = 2[\eta]/5$) was independent of molecular mass, and the dendritic macromolecule behaved more like a constant density particle than a Gaussian or swollen polymer coil. Indeed, recent small-angle neutron and X-ray scattering results by us[10] and others[11−14] have demonstrated that dendritic macromolecules in solution exhibit conformation closer to that of globular particles than the Gaussian coil structures more typical of linear chains.

In addition to size change, dendritic macromolecules can change shape,[15] achieving an aspect ratio of up to 2/1 when interpreted as adopting a cylindrical shape in Langmuir−Blodgett studies. However, some care should be used in making a global assumption that this type of size/shape change is possible with all dendritic macromolecules; dendritic macromolecules with more rigid monomers have been synthesized that show very little size/shape change.[16−18]

Diblock copolymers consisting of both dendritic and linear blocks have received considerable recent attention due to their novel macromolecular structure and unique solution properties.[19−23] One of the driving forces for

* Corresponding author: e-mail mackay@msu.edu; phone 517-432-4495, fax 517-432-1105.

10.1021/ma0204608 CCC: $22.00
Published on Web 09/28/2002

these studies is the potential to combine the novel interfacial properties of dendritic macromolecules with the processability and phase separation behavior of linear polymers. While a significant amount of work has been devoted to the synthesis and solution properties of hybrid dendritic−linear diblock copolymers, only a limited number of papers have been devoted to their solid-state and bulk behavior.[20] These tadpole-like molecules have been shown to exhibit amphiphilic behavior both in solution and in bulk for hydrophilic−hydrophobic systems. As surfactant and linear block copolymer systems show, they can self-assemble into various morphologies from micelles to lamella, depending on the relative block sizes. Most notably, van Hest et al.[19] studied a block copolymer system consisting of linear polystyrene grafted to a poly(propyleneimine) dendrimer in aqueous solution. When the dendrimer generation was increased from 2 to 4, the morphology of the microphase-separated domains changed from bilayers to rods to spheres. Subsequently, the morphology of the same hybrid molecules were studied in their solid state, and a similar dependence of the morphology on the size of the dendritic block was observed.[22] However, the phase separation behavior of dendritic−linear block copolymers, which do not have a strong amphiphilic driving force, has not been studied in detail. As a consequence, only a very limited understanding of the factors affecting phase separation and structure of the resulting nanoscopic domains in these hybrid systems has been developed. It should be mentioned that Gitsov and Fréchet[24] studied similar dendritic−linear polymer systems; however, these results are influenced by crystallization of the linear poly(ethylene glycol) block.

It is the purpose of this study to further explore the novel solid-state behavior of hybrid block copolymers consisting of linear polystyrene grafted to a sixth-generation dendron of poly(benzyl ether). In comparison to previous work, a relatively large dendritic fragment, sixth generation with a molecular mass of 13 464 Da, is employed which more accurately reflects traditional linear block copolymer systems in terms of molecular mass while allowing a more compact, 3-dimensional dendron to be examined. Characterization of the morphologies by TEM and scattering will be used to gain some insight into the molecular conformation. It is anticipated that the branched molecular architecture of the dendron phase will limit the degree of deformation and molecular interpenetration possible in comparison to the linear block. Therefore, comparison of the microstructures observed with those typically found for comparable linear−linear block copolymers will provide insight into the influence of architecture on block copolymer phase behavior.

Experiment

General Methods. Commercial reagents were obtained from Aldrich and used without further purification. Analytical TLC was performed on commercial Merck plates coated with silica gel GF254 (0.24 mm thick). Silica gel for flash chromatography was Merck Kieselgel 60 (230−400 mesh, ASTM). Nuclear magnetic resonance was performed at 25 °C on a Bruker AVANCE 400 FT-NMR spectrometer using deuterated solvents and the solvent peak as a reference. Gel permeation chromatography was performed in tetrahydrofuran (THF, 25 °C, flow rate 1 mL/min) on a Waters chromatograph equipped with four 5 μm Waters columns (300 × 7.7 mm) connected in series with increasing pore size (100, 1000, 100 000, 1 000 000 Å). A Waters 410 differential refractometer and 996 photodiode array detector were employed. The polystyrene molecular weights were calculated relative to linear polystyrene standards.

Bis(tetrahydropyran)-Protected Alkoxyamine (4). NaH (0.468 g, 11.7 mmol, 1.20 equiv) and 18-c-6 (10 mg) were added to a THF (20 mL) solution of the bis(tetrahydropyran)-protected alcohol, **2** (3.00 g, 9.74 mmol). The solution was stirred under argon for 10 min; the chloromethyl derivative (2,2,5-trimethyl-3-(1-(4′-chloromethyl)phenylethoxy)-4-phenylazahexane, **3**)[25] (2.52 g, 6.75 mmol) was added dropwise from a solution of THF (10 mL), and the reaction refluxed for 16 h. The excess sodium hydride was reacted with a small amount of water, and the reaction mixture was extracted (dichloromethane/water). The organic phase was dried with $MgSO_4$ and filtered, and the crude product was purified by column chromatography (flash) eluting with 80/20 dichloromethane/hexane switching to 5/95 Et_2O/dichloromethane to give the protected alkoxyamine, **4**, as a colorless glass (2.72 g, 65.3%). ^{1}H NMR ($CDCl_3$, 400 MHz, both diastereomers): δ 0.24 (d, J = 6.5 Hz, 3H), 0.55 (d, J = 6.5 Hz, 3H), 0.79 (s, 9H), 0.95 (m, 3H), 1.05 (s, 9H), 1.30 (d, J = 7.0 Hz, 3H), 1.54−2.05 (complex m, 30H), 2.35 (two m, 2H), 3.30 (d, J = 10.8 Hz, 1H), 3.34 (d, J = 10.8 Hz, 1H), 3.65 (m, 4H), 3.93 (m, 4H), 4.50 (m, 8H), 4.95 (q + q, 2H, J = 6.5 Hz) 5.32 (t + t, 4H), 6.73 (s, 6H) 7.1−7.4 (m, 18H). ^{13}C NMR ($CDCl_3$, 100 MHz, both diastereomers): δ 18.79, 18.83, 19.75, 21.14, 21.96, 22.17, 23.15, 24.67, 25.24, 25.48, 28.26, 28.41, 30.38, 31.66, 32.02, 60.51, 62.01, 62.89, 71.91, 72.01, 72.22, 82.50, 83.32, 94.65, 96.38, 96.54, 104.42, 104.62, 109.06, 126.16, 126.32, 127.02, 127.19, 127.35, 127.69, 130.94, 137.24, 140.53, 144.42, 158.18, 158.25.

Bis(phenolic) Alkoxyamine (5). The bis(tetrahydropyran)-protected alkoxyamine, **4** (3.20 g, 4.95 mmol), was dissolved in tetrahydrofuran (25 mL), and methanol (ca. 5 mL) was added until the solution became very slightly hazy. *p*-Toluenesulfonic acid (0.75 g, 4.0 mmol) was then added, and the reaction mixture was stirred at room temperature overnight with the reaction being monitored by thin-layer chromatography developing with dichloromethane. Sodium bicarbonate ($NaHCO_3$) was added to terminate the reaction, and the reaction mixture evaporated to dryness. The crude product was purified by column chromatography (flash) eluting with dichloromethane increasing in polarity to 20/80 Et_2O/dichloromethane to give the bis(phenol), **5**, as a colorless glass (2.06 g, 86.1%). ^{1}H NMR ($CDCl_3$, 400 MHz, both diastereomers): δ 0.24 (d, J = 6.5 Hz, 3H), 0.55 (d, J = 6.5 Hz, 3H), 0.79 (s, 9H), 0.95 (m, 3H), 1.05 (s, 9H), 1.30 (d, J = 7.0 Hz, 3H), 1.54 (d, J = 6.8 Hz, 3H), 1.62.9 (d, 3H, J = 6.8 Hz), 2.35 (two m, 2H), 3.30 (d, J = 10.8 Hz, 1H), 3.34 (d, J = 10.8 Hz, 1H), 4.42 and 4.45 (each s, 4H, both diastereomers), 4.55 and 4.60 (each s, 4H, both diastereomers) 4.95 (q + q, 2H, J = 6.5 Hz, both diastereomers) 5.75 (s, 4H, PhOH), 6.23 (s, 3H), 6.40 (s, 6H), 7.1−7.4 (m, 18H). ^{13}C NMR ($CDCl_3$, 62.9 MHz, both diastereomers): δ 21.15, 21.98, 22.18, 23.11, 24.59, 28.26, 28.43, 31.71, 32.03, 60.43, 60.54, 71.46, 71.68, 72.29, 82.45, 83.27, 102.52, 107.64, 126.22, 126.38, 127.19, 127.39, 127.99, 130.94, 131.01, 135.75, 136.36, 140.45, 142.23, 142.44, 144.89, 145.56, 156.87.

Generation-6 Alkoxyamine, [G6]-I, 6. A mixture of the fifth-generation bromide, [G5]-Br, **7** (7.50 g, 1.11 mmol, 2.1 equiv),[26] and the bis(phenolic) alkoxyamine, **5** (0.253 g, 0.529 mmol), K_2CO_3 (5.00 g), and 18-crown-6 (0.1 g) in acetone (100 mL) was heated at reflux for 48 h. The reaction mixture was then evaporated to dryness and redissolved in dichloromethane washed with water, and then the water was extracted with dichloromethane. The combined organic phase was dried with magnesium sulfate ($MgSO_4$), filtered, and evaporated to dryness. The crude product was purified by flash chromatography eluting with 80/20 dichloromethane/hexane gradually increasing in polarity to 5/95 Et_2O/dichloromethane to give the sixth-generation dendron, **6**, as a colorless foam (5.84 g, 78.8%). ^{1}H NMR ($CDCl_3$, 400 MHz, both diastereomers): δ 0.20 (d), 0.55 (d), 0.80 (s), 0.95 (d), 1.05 (s), 1.30 (d), 1.55 (d), 1.65 (d), 4.45 (m), 4.82 and 4.89 (each s), 6.47−6.58 (complex m), 7.22−7.33 (m).

General Procedure for the Preparation of [G-6]-PS, 8. Styrene, or d_8-styrene (1.00 g, 9.6 mmol), and [G-6]-I, **6** (0.50 mg, 0.035 mmol), were placed in an ampule together with a stirrer bar. After three freeze and thaw cycles the ampule was sealed under argon and heated for 8 h at 120 °C. The resulting polymer was dissolved in dichloromethane and purified by precipitation into a 1:1 mixture of 2-propanol/acetone followed by reprecipitation into methanol to give **8** as a colorless powder (1.34 g, 89.6%). ^{1}H NMR ($CDCl_3$, 400 MHz): δ 1.20−2.20 (broad m, aliphatic-H) 4.82 and 4.89 (each s, OCH_2), 6.20−7.40 (complex m, aromatic-H). The degree of polymerization of the linear polystyrene blocks could be simply controlled by the molar ratio of dendritic initiator to monomer.[27] HPLC analysis of the diblock copolymers was performed by normal-phase HPLC using a silica column eluting with a gradient from hexane to THF (1 mL/min, 25 °C) coupled to an ELSD detector. The block copolymer was observed to elute at an intermediate elution volume between polystyrene and the pure dendron.

Sample Preparation. Solid films of the hybrid dendron−deuterated polystyrene block copolymers were produced by slightly different methods for transmission electron microscopy (TEM) and small-angle X-ray scattering (SAXS) than for small-angle neutron scattering (SANS) experiments. For the first two techniques, solid films were prepared by slow evaporation of a ca. 5 wt % benzene solution of the polymer over 10−14 days; further evaporation was performed for a week under vacuum. The samples were subsequently annealed at 160 °C for a week under high vacuum. The samples utilized in SANS experiments were prepared in a similar manner except pellets were produced under pressure after solvent evaporation and annealed for a shorter time (1 h to 1 day) at 170 °C.

Sample Characterization. TEM experiments were conducted with a JEOL 100CX TEM operated at an accelerating voltage of 100 kV. To prepare specimens for TEM, a small piece of sample was microtomed using a Leica Ultracut cryomicrotome with a diamond knife at room temperature to obtain ultrathin (about 40 nm) sections. These were then stained with RuO_4 vapor and observed under TEM. The stain was found to penetrate the dendron containing regions more heavily than those consisting of polystyrene.

The SANS measurements were taken using the 30 m NG3 SANS instrument at the National Institute for Standards and Technology (NIST) Center for Neutron Research (NCNR) in Gaithersburg, MD. Two instrument configurations were used. The first had five guides, a sample-to-detector distance of 3.9 m, and a 20 cm detector offset. The second configuration had one guide, a sample-to-detector distance of 13.0 m, and no detector offset. Both configurations had radiation with a wavelength of 6 Å with a 15% spread. The total wave vector (q) range covered was 0.0039−0.1667 Å^{-1}, where $q = 2\pi \sin \theta/\lambda$ with θ and λ defined as the scattering angle and radiation wavelength, respectively. Measurements were taken at a temperature of 170 °C and at room temperature with little difference seen in the scattering patterns.

SAXS was performed at the University of Massachusetts using Ni-filtered Cu−Kα radiation (1.54 Å wavelength) from a Rigaku rotating anode, operated at 40 kV, 200 mA. The primary beam was collimated by a set of three pinholes. A gas-filled area detector (Siemens Hi-Star), which was located at 879.0 mm from the sample, was used to record scattering patterns. Circular averaging was performed to produce a plot of intensity vs scattering wave vector, q, by using the Siemens General Area Detector Diffraction Software (GADDS) program.

Separate thermodynamic characterization of the dendritic samples[9] revealed the density of G-6 dendron can be accurately represented by 1.151 exp(−5.372 × 10^{-4}[T (°C) − 90]) in g/mL above the glass transition temperature of 45 °C. Literature values[29] for polystyrene were used to find the density which is given by 0.982 exp(−5.824 × 10^{-4}[T (°C) − 140]) in g/mL above the glass transition temperature of 98 °C. (This relation is based on data for 34.5 kDa polystyrene; little change is seen in the volume fractions determined from the polymer bulk densities if different densities for higher mass samples were used in the regression.)

Scattering Calculations. Random, lamellar, and hexagonally close-packed cylinders were found present in the systems studied here. The characteristic scattering distance, d, was calculated through $d = 2\pi/q^*$, where q^* is the local maximum of the intensity with the scattering vector at the smallest vector magnitude used here. One characteristic dimension of the phase-separated structures in a *random morphology* is taken as $\phi^{1/3}d$, where ϕ is the volume fraction of the minor component. The other dimension, due to the major component, is approximated by $d - \phi^{1/3}d$. Polystyrene is the minor component for the system studied here, and so the characteristic dimension of polystyrene and dendritic components are $d_{PS} = \phi_{PS}^{1/3}d$ and $d_D = d - \phi_{PS}^{1/3}d$, respectively, with ϕ_{PS} representing the volume fraction of polystyrene. As there is no long-range order, higher-order peaks in I vs q plots are not evident. The *lamellar morphology* characteristic dimensions are obtained by standard relations $d_D = \phi_D d$ and $d_{PS} = \phi_{PS}d$, with ϕ_D being the dendritic volume fraction. This morphology has a correlation peak reflection at $2q^*$, which is easily discernible in experiments. Relations for *hexagonally close packed cylinders morphology* are found by realizing that d is an interplanar distance. The cylinder-to-cylinder distance, D, is $2d/\sqrt{3}$. The dendron is determined to be the cylinder phase in this study, and so $d_D^2 = [4/\pi]\phi_D D d$ with $d_{PS} = D - d_D$. The correlation peak for this morphology has reflections at $\sqrt{3}q^*$ and $2q^*$.

Results and Discussion

As detailed previously,[30] hybrid dendritic−linear diblock copolymers can be prepared by attachment of a chloromethyl-functionalized alkoxyamine to the hydroxymethyl focal point group of a suitable poly(benzyl ether) dendron followed by nitroxide-mediated living free radical polymerization.[31−33] However, this synthetic approach was only applied to dendrons from generation 1 to 4 and was not considered suitable for the synthesis of hybrid dendritic−linear based on larger dendritic fragments due to the difficulty in preparing higher generation dendrons.[26] An alternative strategy was then adopted on the basis of the previously reported success of using poly(phenolic) derivatives as cores for the synthesis of large dendritic macromolecules.[34] The two phenolic groups of methyl 3,5-dihydroxybenzoate, **1**, were protected with tetrahydropyran groups followed by reduction with lithium aluminum hydride to give the alcohol, **2**. Coupling of the anion of **2** with the chloromethyl alkoxyamine, **3**, then gave the protected initiator, **4**, which could be deprotected in high yield by reaction with *p*-toluenesulfonic acid to afford the desired bis(phenolic) alkoxyamine, **5** (Scheme 1). The advantage of using **5** in the synthesis of the sixth-generation (G6) dendritic initiator, **6**, is the presence of the 3,5-dihydroxybenzyl group which acts as a first-generation core, negating the preparation and use of the corresponding sixth-generation dendritic alcohol. The sixth-generation initiator, **6**, can therefore be prepared from the much more readily accessible fifth-generation bromide, **7**, by alkylation of the diphenol, **5**, under standard Williamson conditions (K_2CO_3/18-c-6) (Scheme 2). Such a strategy avoids a chemical transformation at the sixth generation, but more importantly the separation of [G-5]-Br from [G-6]-I is more easily facilitated than the separation of [G-6]-OH from [G-6]-I.

Polystyrene (PS) blocks of controlled molecular weight could be conveniently grown from **6** under living free radical conditions by reaction with either styrene or deuterated styrene at 120 °C. After purification by precipitation, the hybrid dendritic−linear block copolymer, **8**, was obtained in each case with polydispersities less than 1.1 (Scheme 3). The low polydispersities for

Scheme 1. Synthesis of the Bis(phenolic) Alkoxyamine Initiator, 5

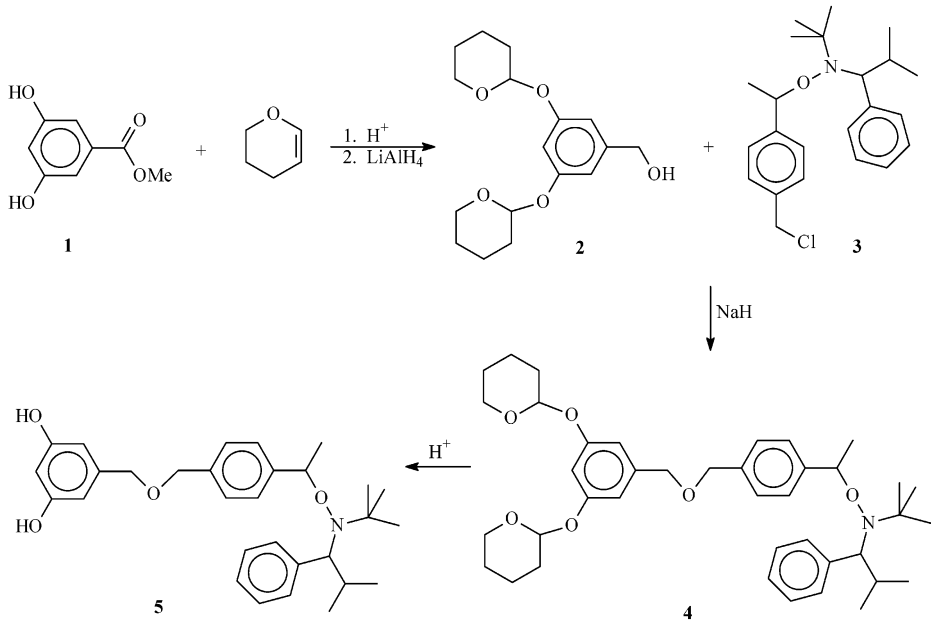

Scheme 2. Synthesis of the Sixth-Generation Alkoxyamine Initiator, 6, from the Diphenol, 5, and [G-5]-Br, 7

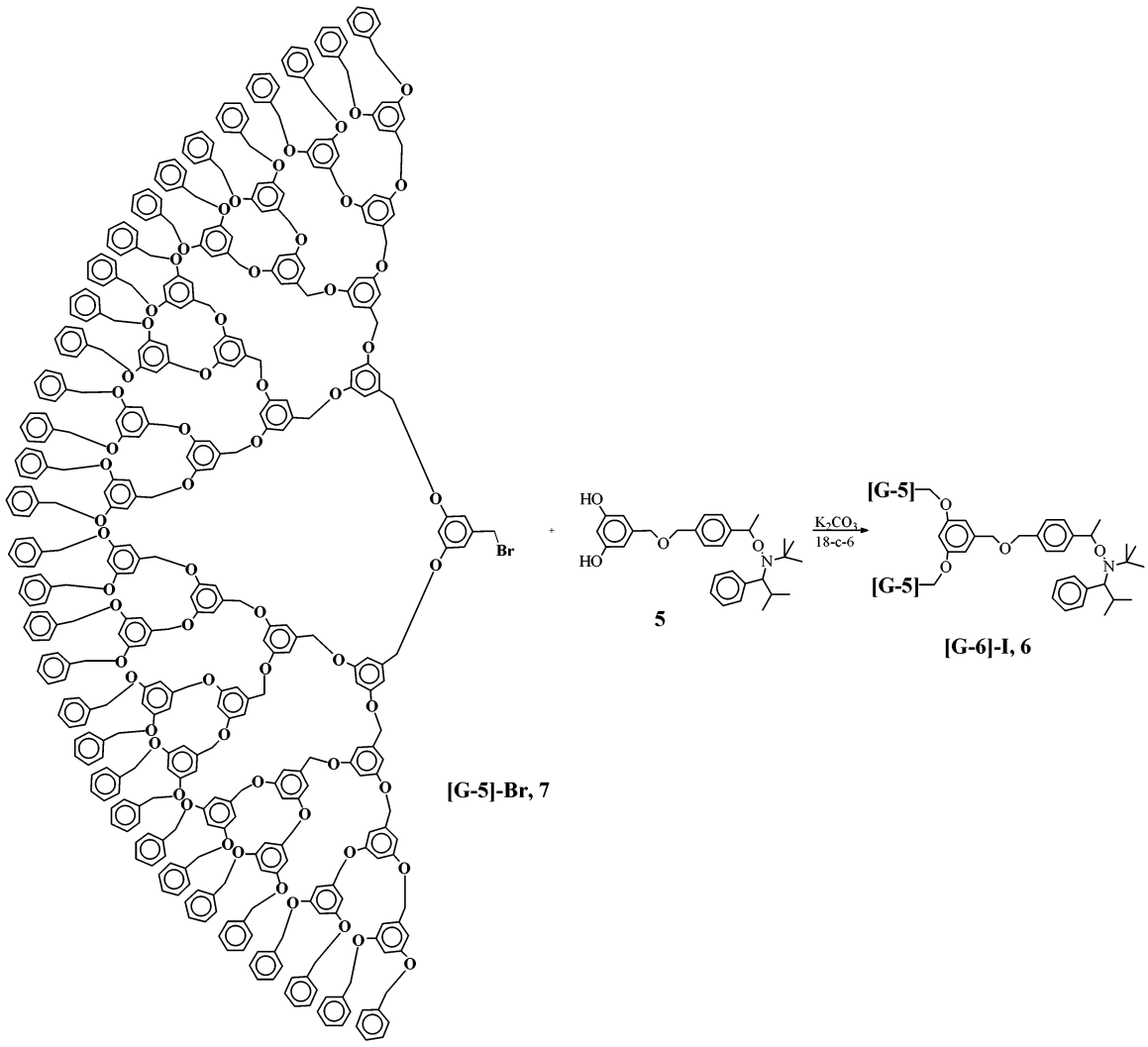

the dendritic initiator, **6**, and the hybrid copolymers, **8**, allowed their purity to be easily determined by GPC and HPLC. In each case, no observable amount of homopolymer impurities was detected. Three main samples were investigated in detail, (G6-PS-20K), (G6-PS-43K), and (G6-PS-74K), and the molecular weight value given, i.e., 20K, is the total molecular weight for the block copolymer. In all the samples, the dendron has a consistent

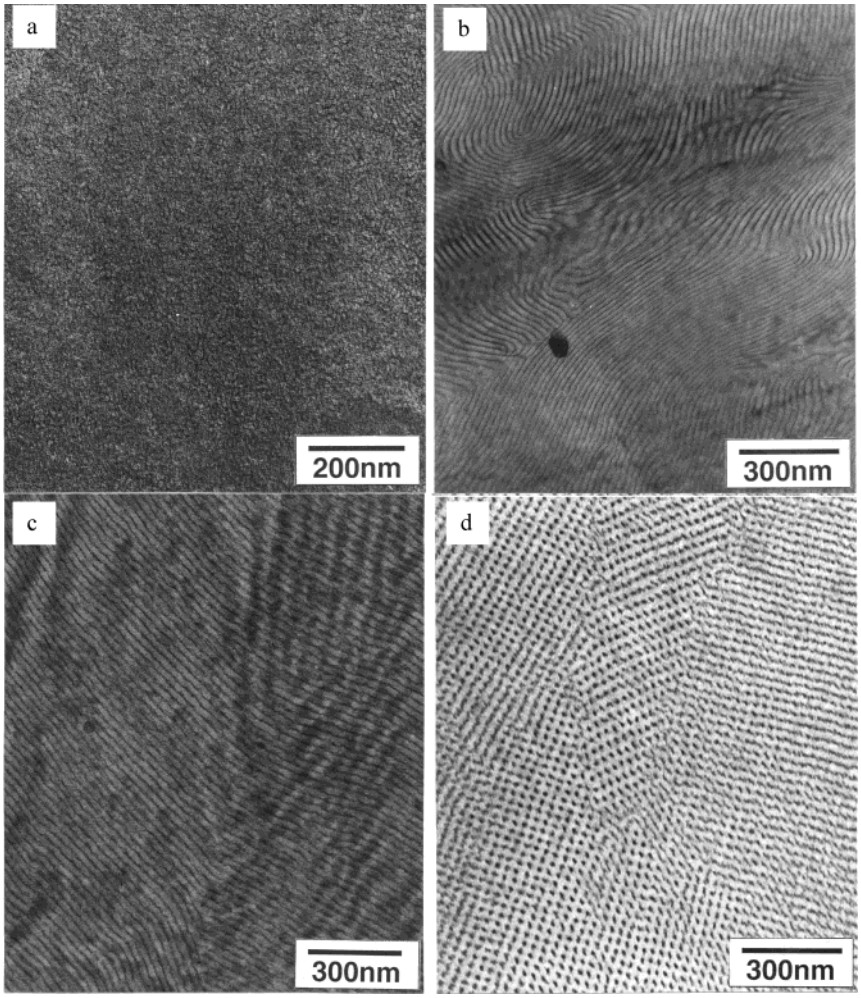

Figure 1. Transmission electron micrographs of sixth-generation poly(benzyl ether) dendron−linear polystyrene block copolymers: (a) G6-PS-20K sample showing random morphology; (b) G6-PS-43K with lamellar morphology and G6-PS-74K with the cylinder morphology viewed parallel to the cylinder axis (c) and perpendicular to the cylinder axis (d).

Scheme 3. Synthesis of Hybrid Dendritic−Linear Block Copolymer, [G-6]-PSt, 8, by Nitroxide-Mediated Living Free Radical Polymerization

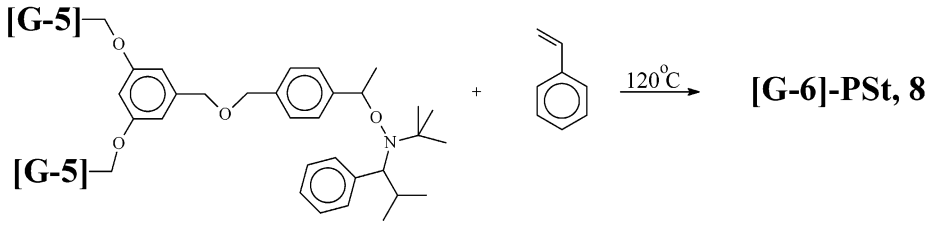

[G-6]-I, 6

molecular weight of 13 464 amu, so for the 20K sample, the linear deuterated (d_8) polystyrene chain has a molecular weight of 6500 amu, which gives a relative dendron percentage of 67%.

Figure 1 shows transmission electron micrographs (TEMs) for the three block copolymers. Stain was preferentially located in the dendron-rich regions, and hence, these regions are darker in color. It is clear that the materials show microphase separation; that is further confirmed by scattering data shown in Figure 2. The small-angle X-ray scattering (SAXS) data for G6-PS-20K have a liquidlike peak characteristic of a disordered morphology with a characteristic length scale (d) of 14.5 nm. The intermediate molecular mass sample, G6-PS-43K, exhibits obvious scattering maxima at q^* and $2q^*$, which is indicative of a lamellar morphology with a repeat distance (d) of 20.5 nm. A cylinder morphology was observed for the highest molecular mass sample, G6-PS-74K, with scattering maxima located at q^*, $\sqrt{3}q^*$, and $2q^*$. This is consistent with hexagonal packing of cylinders with d of 26.7 nm. The small-angle neutron scattering (SANS) data shown in Figure 2 display similar results to the SAXS with d of 29.4 nm. Note there are instrument and wavelength broadening effects in SANS that might lead to a larger spacing; SANS data serve as another experimental technique to clearly demonstrate that the cylinder morphology is well developed. The TEM for this sample

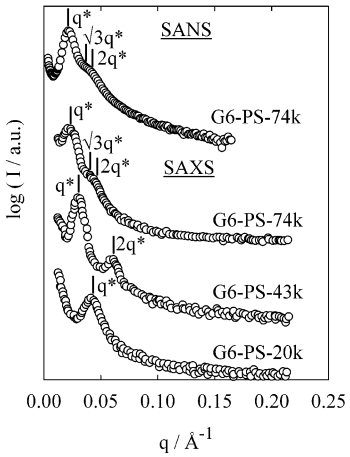

Figure 2. Scattering data, intensity (I) vs scattering vector (q), from the sixth-generation poly(benzyl ether) dendron−linear polystyrene block copolymers. The upper curve is SANS data from G6-PS-74K with the maximum in the scattering vector (q^*) marked. The three lower curves are SAXS data from G6-PS-74K, G6-PS-43K, and G6-PS-20K again with q^* marked. The associated reflections for each morphology are also marked on each curve; see text for details.

also shows that the cylindrical morphology is readily apparent (Figure 1c,d).

The various morphologies of the samples are summarized in Table 1. Also given in this table are the volume fractions for the samples based on polymer bulk densities given above. Different morphologies are present with the dendritic system at equivalent volume fraction to linear−linear block copolymer systems[1] although other block copolymer systems deviate from these phase boundaries to some extent.[35]

It should be noted that these systems are probably in the strong segregation regime. Other experiments showed the copolymers appeared to have degraded at ca. 200 °C when heated in the neutron beam for an extended period, and no order−disorder transition was observed prior to (apparent) degradation in the SANS experiments. Furthermore, samples could be heated to 170 °C, well above the glass transition temperature for PS, and quenched to yield the same microstructure independent of the experimental heating protocol. Interestingly, Jeong et al.[8] determined the solubility parameter difference between poly(benzyl ether) dendrons and PS is at most 0.1 $(\text{cal/cm}^3)^{1/2}$, making χ of order 10^{-4}. As a consequence, the segregation parameter χN is approximately 0.1 for the highest molecular mass sample, and so only weak segregation is expected. This suggests an additional entropic effect associated with the impenetrability of the dendron by the linear chain (see below) as a possible driving force for phase separation. Similar speculations have been proposed for blends of linear and branched molecules by Chen et al.[36] Thus, strong segregation is most likely present in dendritic−linear block copolymers and may be driven through entropic differences between and/or within each block. To gain more insight into this phenomenon, detailed analysis and description of each morphology are given below and summarized in Table 1.

Cylinder Morphology. Gido and Wang[35] surveyed the morphology literature for linear−linear block copolymers. From these data we find the hexagonally close-packed cylinder morphology is developed when the minor component has a volume fraction of 0.27 ± 0.07 with minimum and maximum values of 0.14 and 0.39, respectively. Dendron cylinders are found when the dendritic volume fraction is 0.16 (see Table 1), and so this value is not outside the minimum found for linear−linear systems; however, it is quite low. Note Román et al.[22] showed the cylinder morphology develops when the dendron mass fraction is 0.13, and so this may indicate that molecular architecture plays a significant role in the phase boundaries, which will become clearer below.

To investigate the morphological details, the size of the dendritic and linear polymer blocks must be estimated. The radius of gyration for polystyrene (R_g(PS)) is found from the relation developed by Cotton et al.[37] $R_g(\text{PS})/\text{nm} = 0.870\sqrt{(M_{PS}/\text{kDa})}$, where M_{PS} is the polystyrene molecular mass.

The R_g for G6 monodendron (R_g(D)) in d_6-benzene is 1.95 ± 0.04 nm, while the viscosimetric radius (R_η, $[\eta] \equiv [10/3]\pi R_\eta^3 N_A/M$; $[\eta]$ is the intrinsic viscosity, N_A Avogadro's number, and M molecular mass) in benzene is 1.65 nm.[10] Note a constant density sphere should have $R_g/R_\eta = \sqrt{(3/5)} \sim 0.77$, and the above results are contrary to the calculated ratio. Results in tetrahydrofuran (THF) solvent[10] reveal that the higher generation monodendrons tend toward the constant density sphere result for this solvent with $R_\eta = 2.2$ nm for G6 (scattering data in this solvent only extended to fifth generation; the value of R_η is from Mourey et al.[38]). Also, Jeong et al.[8] determined third- to fifth-generation (G3−G5) poly(benzyl ether) monodendrons dissolved in chloroform had a molecular mass (M) independent intrinsic viscosity, $[\eta] = 2.6$ mL/g. This is indicative of constant density spheres since $[\eta] = {}^5/_2\rho_m{}^{-1}$, where ρ_m is the single molecule density. Since the density is constant, then R_η is expected to scale with $M^{1/3}$, and one can find R_η to be 1.8 nm for G6. These results also demonstrate the capability of poly(benzyl ether) monodendrons to change size. It is clear that solvent effects are significant in determining the monodendron size and that the molecular conformation can be affected to create constant density spheres in the expanded form (THF, $R_\eta = 2.2$ nm) or the collapsed form (chloroform, $R_\eta = 1.8$ nm). We take the R_g of G6 monodendron as 2 nm in calculations given below and recognize this is an approximation that does not significantly influence our conclusions.

The ratio of the half-characteristic distance for polystyrene ($R_{PS} = d_{PS}/2$) to $2R_g$(PS) in the cylinder morphology is close to one as shown in Table 1. Slight distortion of the polystyrene chain is expected. This is contrary to the ratio for the dendron cylinders with $R_D/2R_g(D)$ equal to ∼2, and significant distortion is likely.

To obtain cylinders, almost 2 times greater in diameter than the globular dendron, the molecules must therefore undergo a significant shape change. Kampf et al.[15] found dendrons can change shape at an interface and interpreted them in terms of a cylinder with a length on diameter ratio of 2/1, which is a clear deviation from a spherical architecture. Rather than assume a cylindrical shape as that postulated by Kampf et al., the dendrons in the cylinder phase-separated morphology are assumed to arrange in a conformation to approximate a circular segment with thickness L_D (akin to a piece of pie with radius R_D and thickness L_D, see Figure 3). The individual dendron molecular volume is taken as $\pi R_D{}^2 L_D/N$ for N dendrons distributed around the cylinder ("N" pieces of pie). Assuming negligible dendron volume change, this volume can be equated to

Table 1. Radiation Scattering Data, SAXS and SANS, for the Hybrid Block Copolymers Designated by Sample Code in the First Column[a]

polymer	M_{PS}, kDa	w_D (ϕ_D)	q^*, Å^{-1}	R_{PS}, R_g(PS), nm	$R_{PS}/2R_g$(PS)	R_D, $R_g(D)$, nm	$R_D/2R_g(D)$	morphology
G6-PS-20K[b]	6.54	0.67 (0.64)	0.0433	4.7, 2.2	1.1	2.6, 2.0	0.65	random
G6-PS-43K[b]	29.5	0.31 (0.29)	0.0306	6.9, 4.7	0.73	3.4, 2.0	0.85	lamellar
G6-PS-74K[b]	60.5	0.18 (0.16)	0.0235	8.3, 6.8	0.61	7.1, 2.0	1.8	D-cylinders
G6-PS-74K[c]	60.5	0.18 (0.16)	0.0214	9.2, 6.8	0.68	7.8, 2.0	2.0	D-cylinders

[a] The sixth-generation (G6) dendron molecular mass is constant for all copolymers and equal to 13 464 Da, only the polystyrene mass (M_{PS}) changes as shown in the second column. The relative mass (w_D) and volume (ϕ_D) fractions are given in the third column, and q^* is shown in the following column. The half characteristic size in the bulk sample for polystyrene ($R_{PS} = d_{PS}/2$) and the radius of gyration for polystyrene (R_g(PS)) are given in the fifth column followed by the ratio $R_{PS}/2R_g$(PS) in the sixth column. Similar parameters for the dendron are given in the following two columns with the final column giving the morphology; random, lamellar, or dendron cylinders in a hexagonally close-packed arrangement, D-cylinders. [b] SAXS measurements. [c] SANS measurements.

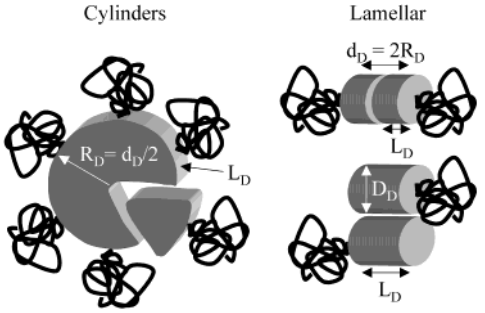

Figure 3. Cartoon demonstrating the arrangement of dendrons in the hexagonally close-packed cylinder morphology with nominally six dendritic fragments per cylindrical repeat unit (left) or in the lamellar morphology (right). Appropriate dimensions are given in the cartoons; see text for details.

that for a single molecule sphere ($4\pi R_g(D)^3/3$) to arrive at

$$L_D/R_D = [4N/3]\{R_g(D)/R_D\}^3$$

The value of N is unknown, and a detailed calculation would need to be performed to balance energies associated with dendron and polystyrene conformations, as well as the interfacial energy; here we assume N is 6 or 12. Using R_g/R_D from Table 1, the ratio L_D/R_D is found to be ∼0.15−0.35. We hypothesize this conformation is possible on the basis of the abovementioned work which demonstrated the shape changing capabilities of poly(benzyl ether) dendrons. In addition, dendritic macromolecules have been observed to assemble into a cylindrical morphology before by Hudson et al.[39] in addition to the previously cited work.[22] Furthermore, Hudson et al. hypothesize structures similar to what we have discussed above with six dendritic macromolecules assembling into a columnar morphology albeit for a first-generation, relatively flat dendron (Figure 3). Thus, on the basis of this work, we believe substantial dendron shape change is necessary to achieve the cylinder morphology.

The inherent assumption of the above calculation is that dendron−dendron interpenetration is minimal. To justify this assumption, we first note the bulk density of G6 dendron is approximately 1.2 g/mL at room pressure and temperature[9] while the single molecule density in the collapsed state (chloroform) is ∼1.0 g/mL ($\rho_m = {}^5/_2[\eta]^{-1}$). Thus, very little intermolecular interpenetration is necessary for the bulk density to be achieved. This is in sharp contrast to linear polymers; $[\eta]$ for polystyrene in a Θ solvent[40] follows 2.6 M (kDa)$^{1/2}$ in mL/g yielding a single molecule density of 0.26 g/mL for a molecular mass equivalent to G6. Since the bulk density is ca. 1.0 g/mL, much more significant molecular interpenetration is necessary to achieve this density. Second, Farrington et al.[41] and Hawker et al.[42] have shown that dendritic macromolecules follow the Rouse scaling law for the terminal viscosity up to extremely high molecular masses (∼100 kDa). The Rouse law occurs when molecular entanglements are not present, and so this is believed to be the case for dendrons, suggesting again that intermolecular penetration is limited.

Table 2. Morphologies Developed by the Dendron−Linear Polymer System Studied Here Compared to Those Found in the Work of Román et al.[22] [a,b]

polymer	w_D	morphology	polymer	w_D	morphology
G6-PS-20K	0.67	random			
			G5-PS-7.6K[c]	0.58	random
			G4-PS-5.3K[c]	0.40	lamellar
G6-PS-43K	0.31	lamellar			
			G3-PS-4.3K[c]	0.25	lamellar
G6-PS-74K	0.18	D-cylinders			
			G2-PS-3.7K[c]	0.13	D-cylinders

[a] Note the progression of morphology does not depend on dendron type, dendron generation, or molecular mass; the mass (volume) fraction of dendron appears to be the primary variable in determining the morphology. [b] The columns are polymer sample code, mass fraction of dendron (w_D), and morphology developed. [c] Data of Román et al.[22] The sample codes for Román et al.'s materials are for second (G2) to fifth (G5) generation poly(propyleneimine) dendron blocks bonded to the same mass linear polystyrene block (3.2 kDa). The code G5-PS-7.6K indicates a fifth-generation dendron bonded to the polystyrene block to produce a total molecular mass of 7.6 kDa.

Lamellar Morphology. This morphology develops when the dendron volume fraction is 0.29 for the G6-PS43K system. Analysis of a significant amount of data[35] shows the lamellar morphology in linear−linear block copolymer systems is generated when the volume fraction is 0.50 ± 0.10 with low and high volume fractions of 0.36 and 0.72, respectively. Thus, the volume fraction of 0.29 for the dendron−linear system is outside this volume fraction range.

In fact, a lamellar morphology is present at lower mass fraction in the dendritic poly(propyleneimine)−linear polystyrene system studied by Román et al.[22] as shown in Table 2. The dendron bulk density is probably 1.1−1.3 g/cm^3 for this system,[43] making the volume fraction even lower, approximately 0.2. Dendrons appear to significantly affect the phase boundary for the lamellar morphology and thus develop at a volume fraction smaller than expected. This may be a useful characteristic, allowing a linear polymer to be assembled into lamellar morphology when it is the major component by far.

The ratios $R_{PS}/2R_g$(PS) and $R_D/2R_g$(D) are close to one in this morphology, indicating slight chain stretch for

the linear macromolecule and slight shape change for the globular macromolecule. Modeling the dendron as a circular prism (see Figure 3) with base diameter D_D and height L_D yields

$$L_D/D_D = [\sqrt{3}/4]\{L_D/R_g(D)\}^{3/2}$$

by equating the circular prism volume to the molecular volume based on R_g similar to above. Letting L_D equal R_D (dendron spans half the phase-separated structure) or d_D (dendron spans the structure) finds L_D/D_D values of 0.96 and 2.7, respectively. Modeling the dendron as a square prism under the same condition yields an aspect ratio of 1.1 ($L_D = R_D$); thus, if the dendron spans half its lamellar spacing, an aspect ratio near one is expected and minimal shape change (stretching) is expected. Again, detailed modeling is required to determine whether the dendron extends through its entire lamellar spacing; however, minimal shape change would be required if $L_D = R_D(d_D/2)$.

Random Morphology. Reducing the PS block content further ($w_D = 0.67$) results in a microphase-separated material without long-range order (G6-PS-20K). The geometry consistent with the observed TEM and SAXS data is microphase-separated lamellae without long-range order. This morphology exhibits a characteristic spacing, d, of 14.5 nm and d_{PS} and d_D values of 9.4 and 5.2 nm, respectively (see Table 1). It is difficult to make firm conclusions about this morphology due to its lack of long-range order except that it occurs with minor distortion in the dendron block shape expected ($R_D/2R_g(D) = 0.65$, see Table 1). Román et al.[22] found a random morphology at lower dendron mass fraction ($w_D = 0.58$, see Table 2). Thus, this less perfect morphology appears to be independent of dendron chemical type and is present when dendritic macromolecule is the major component.

Conclusion

We have shown that hybrid dendritic−linear diblock copolymers exhibit strong microphase separation, with a progression from ordered cylinder to ordered lamellar and then disordered lamellar phases with decreasing linear block fraction. This behavior is similar to the work of Román et al.,[22] who observed a corresponding morphological transition in a chemically dissimilar amphiphilic hybrid block copolymer system. In our system, the hybrid structure consists of blocks with a solubility parameter difference of, at most, 0.1 (cal/cm^3)$^{1/2}$, and so enthalpic contributions to phase separation are minor, suggesting that this morphological behavior is common for dendritic−linear systems.

Significant dendron shape distortion is required to accommodate the dendron−cylinder geometry. We have justified the shape change through realization that the individual molecule densities are almost equivalent to the bulk, suggesting little intermolecular penetration. In fact, the shape changing ability of dendritic macromolecules is considered a key molecular feature in morphology development. It is also clear from our work that dendrons do influence the phase boundaries when, for example, the lamellar morphology is developed. Thus, molecular architecture can play a key role in assembling a given morphology under conditions that may not be possible with a linear−linear block copolymer. Further, it may be interesting to use a dendron that is relatively inflexible[16−18] or change the dendritic core that in turn influences conformation[44] to manipulate the morphology. This may introduce another variable in addition to volume fraction and molecular architecture for the identification and manipulation of unusual microphase separation.

Acknowledgment. Partial support for this project to M.E.M. through NSF-CTS-0098132 is gratefully acknowledged. N.J.W. and B.M.T. acknowledge funding from DuPont CR&D. M.E.M.. M.J., N.J.W., and B.M.T. gratefully acknowledge a grant from National Institute of Standards and Technology to perform SANS measurements with the help of Drs. C. Glinka and D. Ho. Financial support from the MRSEC Program of the National Science Foundation under Award DMR-9808677 for the Center for Polymeric Interfaces and Macromolecular Assemblies and the IBM Corporation is also gratefully acknowledged.

References and Notes

(1) Bates, F. S. *Science* **1991**, *251*, 898.
(2) Spontak, R. J.; Alexandridis, P. *Curr. Opin. Colloid Polym. Sci.* **1999**, *4*, 140.
(3) Olmsted, P. R.; Milner, S. T. *Macromolecules* **1998**, *31*, 4011.
(4) Lee, C.; Gido, S. P.; Pitsiklis, M.; Mays, J. W.; Tan, N. B.; Trevino, S. F.; Hadjichristidis, N. *Macromolecules* **1997**, *30*, 3732.
(5) Trollsås, M.; Kelly, M. A.; Claesson, H.; Siemens, R.; Hedrick, J. L. *Macromolecules* **1999**, *32*, 4917.
(6) Hedrick, J. L.; Trollsås, M.; Hawker, C. J.; Atthoff, B.; Claesson, H.; Heise, A.; Miller, R. D.; Mecerreyes, J. R.; Dubois, P. *Macromolecules* **1998**, *31*, 8691.
(7) Grayer, V.; Dormidontova, E. E.; Hadziioannou, G.; Tsitsilianis, C. *Macromolecules* **2000**, *33*, 6330.
(8) Jeong, M.; Mackay, M. E.; Hawker, C. J.; Vestberg, R. *Macromolecules* **2001**, *34*, 4927.
(9) Hay, G.; Mackay, M. E.; Hawker, C. J. *J. Polym. Sci., Part B: Polym. Phys.* **2001**, *39*, 1766.
(10) Tande, B. M.; Wagner, N. J.; Mackay, M. E.; Hawker, C. J.; Vestberg, R.; Jeong, M. *Macromolecules* **2001**, *34*, 8580.
(11) Tropp, A.; Bauer, B. J.; Klimash, J. W.; Spindler, R.; Tomalia, D. A.; Amis, E. J. *Macromolecules* **1999**, *32*, 7226.
(12) Tropp, A.; Bauer, B. J.; Prosa, T. J.; Scherrenberg, R.; Amis, E. J. *Macromolecules* **1999**, *32*, 8923.
(13) Poetschke, D.; Ballauff, M.; Lindner, P.; Fischer, M.; Voegtle, F. *Macromolecules* **1999**, *32*, 4079.
(14) Poetschke, D.; Ballauff, M.; Lindner, P.; Fischer, M.; Voegtle, F. *Macromol. Chem. Phys.* **2000**, *201*, 330.
(15) Kampf, J. P.; Frank, C. W.; Malmström, E. E.; Hawker, C. J. *Langmuir* **1999**, *15*, 227.
(16) Devadoss, C.; Bharathi, P.; Moore, J. S. *J. Am. Chem. Soc.* **1996**, *118*, 9635.
(17) Wiesler, U.-M.; Weil, T.; Müllen, K. Nanosized polyphenylene dendrimers. In *Dendrimers III*; Vögtle, F., Ed.; Springer-Verlag: New York, 2001; pp 1−40.
(18) Weil, T.; Wiesler, U. M.; Herrmann, A.; Bauer, R.; Hofkens, J.; De Schryver, F. C.; Müllen, K. *J. Am. Chem. Soc.* **2001**, *123*, 8101.
(19) van Hest, J. C. M.; Delnoye, D. A. P.; Baars, M. W. P. L.; van Genderen, M. H. P.; Meijer, E. W. *Science* **1995**, *268*, 1592. (b) van Hest, J. C. M.; Delnoye, D. A. P.; Baars, M.; Elissen Roman, C.; van Genderen, M. H. P.; Meijer, E. W. *Chem.—Eur. J.* **1996**, *2*, 1616.
(20) Chapman, T. M.; Hillyer, G. L.; Mahan, E. J.; Shaffer, K. A. *J. Am. Chem. Soc.* **1994**, *116*, 11195.
(21) Iyer, J.; Fleming, K.; Hammond, P. T. *Macromolecules* **1998**, *31*, 8758. Iyer, J.; Fleming, K.; Hammond, P. T. *Langmuir* **1999**, *15*, 7299.
(22) Román, C.; Fischer, H. R.; Meijer, E. W. *Macromolecules* **1999**, *32*, 5525.
(23) Johnson, M. A.; Santini, C. M. B.; Iyer, J.; Satija, S.; Ivkov, R.; Hammond, P. T. *Macromolecules* **2002**, *35*, 231.
(24) Gitsov, I.; Wooley, K. L.; Hawker, C. J.; Ivanova, P. T.; Fréchet, J. M. J. *Macromolecules* **1993**, *26*, 5621. (b) Gitsov, I.; Fréchet, J. M. J. *Macromolecules* **1994**, *27*, 7309.
(25) Benoit, D.; Chaplinski, V.; Braslau, R.; Hawker, C. J. *J. Am. Chem. Soc.* **1999**, *121*, 3904. (b) Dao, J.; Benoit, D.; Hawker, C. J. *J. Polym. Sci., Part A: Polym. Chem.* **1998**, *36*, 2161.

(26) Hawker, C. J.; Fréchet, J. M. J. *J. Am. Chem. Soc.* **1990**, *112*, 7638.
(27) Hawker, C. J. *J. Am. Chem. Soc.* **1994**, *116*, 11185.
(28) Deleted in proof.
(29) Zoller, P.; Walsh, D. J. *Standard Pressure−Volume−Temperature Data for Polymers*; Technomic Publishing: Lancaster, 1995.
(30) Leduc, M.; Hawker, C. J.; Dao, J.; Fréchet, J. M. J. *J. Am. Chem. Soc.* **1996**, *118*, 11111.
(31) Hawker, C. J.; Bosman, A. W.; Harth, E. *Chem. Rev.* **2001**, *101*, 3661.
(32) Rodlert, M.; Harth, E.; Rees, I.; Hawker, C. J. *J. Polym. Sci., Polym. Chem.* **2000**, *38*, 4749.
(33) Pasquale, A. J.; Long, T. E. *J. Polym. Sci., Polym. Chem.* **2001**, *39*, 216. Tsoukatos, T.; Pispas, S.; Hadjichristidis, N. *J. Polym. Sci., Polym. Chem.* **2001**, *39*, 320.
(34) Wooley, K. L.; Hawker, C. J.; Fréchet, J. M. J. *J. Am. Chem. Soc.* **1991**, *113*, 4252.
(35) Gido, S. P.; Wang, Z.-G. *Macromolecules* **1997**, *30*, 6771.
(36) Chen, Y. Y.; Lodge, T. P.; Bates, F. S. *J. Polym. Sci., Part B: Polym. Phys.* **2000**, *38*, 2965.
(37) Cotton, J. P.; Decker, D.; Benolt, H.; Farnoux, B.; Higgins, J.; Jannink, G.; Ober, R.; Picot, C.; des Cloizeaux, J. *Macromolecules* **1974**, *7*, 863.
(38) Mourey, T. H.; Turner, S. R.; Rubenstein, M.; Fréchet, J. M. J.; Hawker, C. J.; Wooley, K. L. *Macromolecules* **1992**, *25*, 2401.
(39) Hudson, S. D.; Jung, H.-T.; Percec, V.; Cho, W.-D.; Johansson, G.; Ungar, G.; Balagurusamy, V. S. K. *Science* **1997**, *278*, 449.
(40) Brandrup, J.; Immergut, E. H. *Polymer Handbook*, 3rd ed.; John Wiley & Sons: New York, 1989.
(41) Farrington, P. J.; Hawker, C. J.; Fréchet, J. M. J.; Mackay, M. E. *Macromolecules* **1998**, *31*, 5043.
(42) Hawker, C. J.; Farrington, P. J.; Mackay, M. E.; Wooley, K. L.; Fréchet, J. M. J. *J. Am. Chem. Soc.* **1995**, *117*, 4409.
(43) Bodnar, I.; Silva, A. S.; Deitcher, R. W.; Weisman, N. E.; Kim, Y. H.; Wagner, N. J. *J. Polym. Sci., Part B: Polym. Phys.* **2000**, *38*, 857.
(44) Matos, M. S.; Hofkens, J.; Verheijen, W.; de Schryver, F. C.; Hecht, S.; Pollack, K. W.; Fréchet, J. M. J.; Forier, B.; Dehaen, W. *Macromolecules* **2000**, *33*, 2967.

MA0204608